SUPPORTING INFORMATION

Title: Towards Defining Plasma Treatment Dose: The Role of Plasma Treatment Energy of Pulsed-Dielectric Barrier Discharge in Dictating *in vitro* Biological Responses

Abraham Lin[1,2*], Eline Biscop[1,2], Yury Gorbanev[1], Evelien Smits[2] and Annemie Bogaerts[1]

_____

[1] PLASMANT-Research Group, University of Antwerp, Antwerp, Belgium

[2] Center for Oncological Research—Integrated Personalized & Precision Oncology Network (IPPON), University of Antwerp, Antwerp, Belgium

*Abraham Lin,

Email: Abraham.lin@uantwerpen.be

_____

1 WET AND DRY WELL FOR POWER MEASUREMENTS

Cells were cultured in polystyrene plates that have been processed to make the surfaces hydrophilic. It is well known that untreated plates do not support cell attachment. Based on visual assessment, no aggregates or clusters are seen, in the wet well, and the PBS is spread evenly across the bottom (Figure S1).



Figure S1. An image of a wet well (left) shows no visible aggregates in the well compared to the dry well (right).

2 INCREASED PULSE-FREQUENCY AND TREAMENT TIME REDUCED CANCER CELL SURVIVAL

It is well documented that increasing pulsed-DBD plasma treatment intensity by increasing pulse frequency or treatment duration will reduce cancer cell survival. We also demonstrated this with our DBD plasma system by treating three cancer cell lines at a 1 mm gap distance. Analysis was performed in the same way as described in the methods, using the Trypan Blue exclusion test. It was clear that when treatment time was fixed at 10 seconds, cancer cell survival decreased when exposed to a DBD plasma at higher pulse frequencies (Figure S2a). At both 50 Hz (Figure S2b) and 500 Hz (Figure S2c) treatment, it was also apparent that increasing treatment time resulted in a decrease in cancer cell survival. Altogether, this further supported our reasoning that cancer cell survival is dependent on the delivered plasma energy, and not on a single parameter.

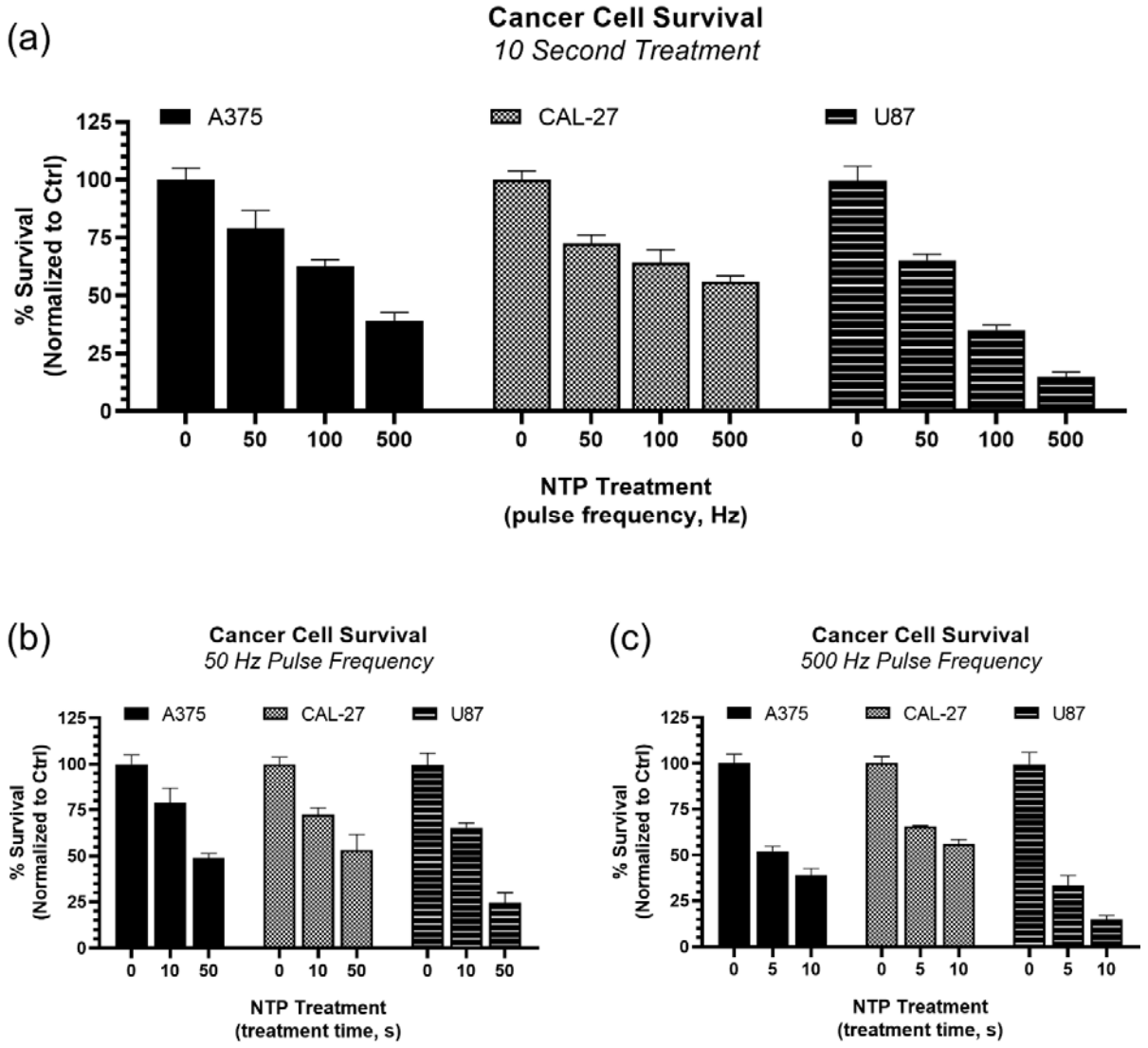


Figure S2. Increasing DBD plasma treatment intensity by increasing pulse frequency or treatment duration reduced cancer cell survival. a) Treatment time was fixed at 10 seconds, and cells were exposed to plasma with a range of pulse frequencies. The DBD plasma pulse frequency was also fixed at b) 50 Hz or c) 500 Hz and cells were exposed to plasma for different times. Our data are in-line with past reports. Data here are represented as mean ± SEM (n=3)

3 CALRETICULIN ANALYSIS WITH SECOND DBD PLASMA SYSTEM

In recent years, the ability of DBD plasma to induce immunogenic cancer cell death (ICD) and increase tumor immunogenicity has garnered heavy attention [8, 14-16]. Induction of ICD is

characterized by several events including the secretion of adenosine triphosphate and surface exposure of calreticulin (CRT) [17, 18]. This modality of cell death is attractive for cancer immunotherapy, as these events could assist a patient's own immunity cycle to mount an effective anti-cancer response.

We have previously demonstrated that DBD plasma treatment induced ICD and elicited CRT exposure on melanoma cell lines, A375 and B16F10 [8]. Cell survival decreased and CRT exposure increased for both cell lines, in equivalent amounts, with higher treatment intensities. In those studies, the DBD electrode was positioned 1 mm above the cells, treatment time was fixed at 10 seconds, and a range of pulse frequencies was used. Here, using the same DBD plasma system, we investigated whether a fixed number of pulses could also induce equivalent CRT emission, independent of pulse frequency and treatment time alone.

The two melanoma cell lines used in our previous report [8], A375 (human) and B16F10 (murine), were treated at equivalent energies by delivering 5000 pulses of DBD plasma and analyzed for CRT 24 hours afterwards with flow cytometry.

3.1 CRT Staining Method

CRT analysis was performed 24 hours after DBD plasma treatment and was measured using a dual staining of propidium iodide (PI) and a monoclonal CRT antibody. Cells were washed with PBS, detached with 200 µL of Accutase, and washed twice with 2 mL of FACS buffer (500 mL sheath fluid (BD Biosciences, 342003) + 2 g bovine serum albumin (Sigma, A9418) + 1 g NaN3 (Merck, 1.06688.0100) in 100 mL H_2O). Each sample was divided into two vials for CRT staining (monoclonal primary rabbit anti-CRT antibody, ab196158, Abcam) or isotype staining (rabbit IgG, monoclonal isotype control, ab199091, Abcam). Cells were stained for 40 min at 4°C and then washed once with FACS buffer. 0.5 µL of PI (556463, BD) was added to each sample

immediately before quantification with flow cytometry (AccuriTM C6, BD). 15000 events were collected and only PI^- cells were analysed for CRT expression.

The collected cell population was gated on morphology, based on forward scatter area (FSC-A) and side scatter area (SCC-A). Within this population, cells were gated on the live population, based on the PI staining (PI─ population). CRT analysis was only performed on the live cell population to avoid non-specific staining of dead/permeabilized cells. The CRT positive gate (CRT+) was set, based on the isotype of the untreated control, and this was uniformly applied to cells in every condition. The percentage of CRT positive (% CRT+) cells for each condition reported here is the % CRT+ population of each condition, minus that of its corresponding isotype, thus accounting for non-specific binding. This gating strategy, applied to A375 cells, is shown in Figure S3a.

3.2 Energy Dependence of DBD Plasma Treatment on Cancer Immunogenicity─Calreticulin Exposure

Following exposure to DBD plasma, a rightward shift was observed in the CRT histograms compared to the untreated for both melanoma cell lines (Figure S3b, c). The percentage of CRT positive cells was determined based on a uniform gating strategy for each cell line and comparison to its corresponding isotype control (Figures S3a). For the A375 cell line, all the DBD plasma treatment conditions elicited a statistically significant increase in surface CRT compared to untreated controls except for one (50 Hz, 100 s; P=0.08) (Figure S3d). For the B16F10 cell line, all treatment conditions at equivalent energies resulted in a statistically significant increase in CRT emission (Figure S3e). Furthermore, no difference was measured between the different conditions (e.g. pulse frequencies and treatment times) when the delivered plasma pulses were held constant (Figure S3d, e).

Taken together, it is clear that not only is total plasma energy important for reducing cell survival, but it also contributes to ICD and potentially other biological readouts.

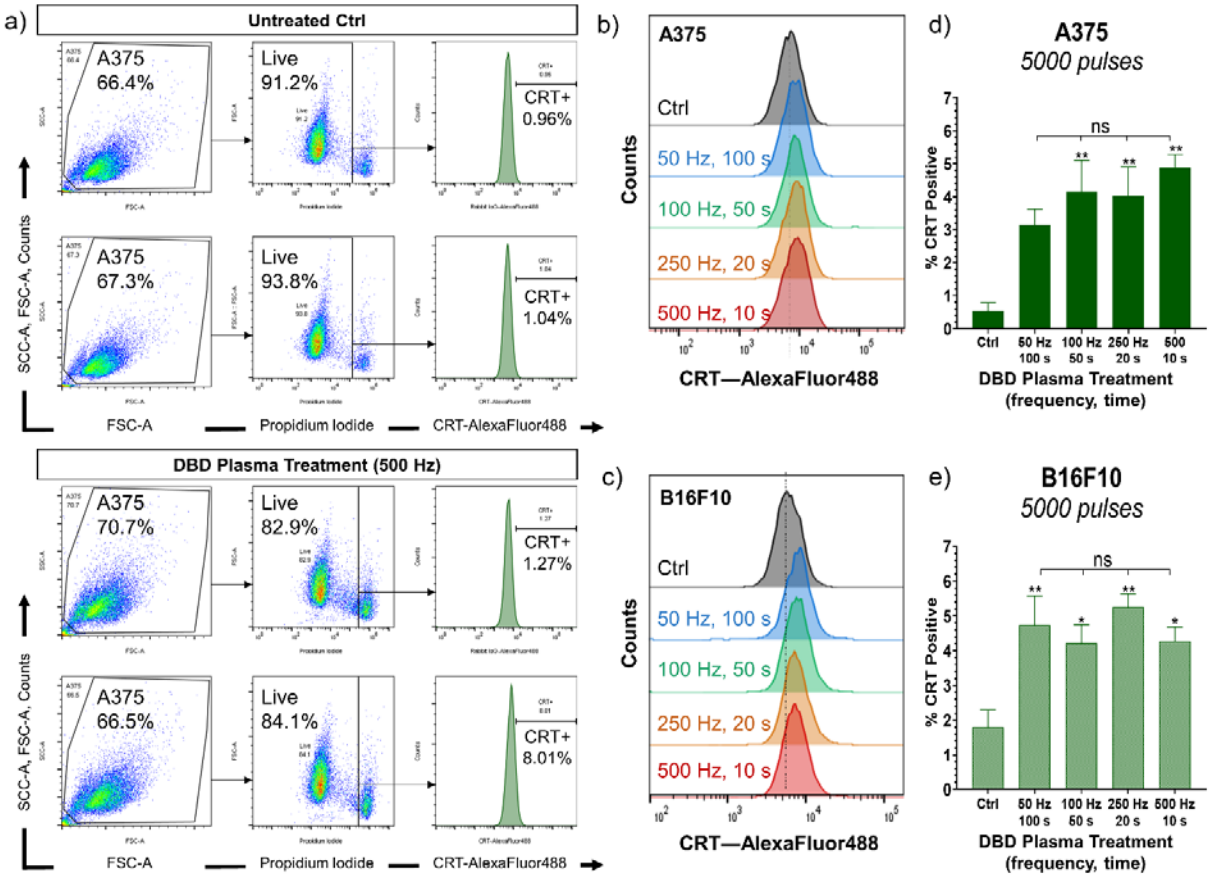


Figure S3. Melanoma cells analyzed for CRT (a hallmark of ICD) following DBD plasma treatment. a) Gating strategy for surface CRT expression on A375 melanoma cells. The top row of each condition (Untreated Ctrl or DBD Plasma Treatment) is of the isotype staining and the bottom row is that of the CRT staining. Histograms of CRT staining showed a rightward shift following DBD plasma treatment compared to control for both b) A375 (n=4-8) and c) B16F10 (n=4-5) melanoma cell lines. The dotted line represents the peak intensity of the untreated controls. Quantification of the CRT signal for both d) A375 and d) B16F10 cells showed that DBD plasma treatment increased CRT exposure compared to untreated controls, but no statistically significant differences were observed between the conditions (e.g. pulse frequency, treatment time), when the number of delivered plasma pulses were held constant. All treatment conditions were compared to each other to determine statistical significance. ns, $P \geq 0.05$; *, $P \leq 0.05$; **, $P \leq 0.001$ (generalized linear mixed model, Tukey's test). Data here are represented as mean ± SEM.

4 RONS MEASUREMENTS WITH SECOND DBD PLASMA SYSTEM

4.1 RONS Measurement Methods

4.1.1 H_2O_2

A potassium bis(oxolato)oxotitanate(IV) dehydrate dihydrate ($K_2[TiO(C_2O_4)_2]•2H_2O$; 89620, Alfa Aesar) solution in H_2O and H_2SO_4 (258105M, Sigma-Aldrich) was used to detect H_2O_2 as adapted from our previous works. DBD plasma-treated PBS was measured in quartz cuvettes (10 mm light path, 2 mm internal width) with a spectrophotometer (Genesys 6, Thermo Fischer). 0.354 g of K2[TiO(C2O4)2]×2H2O was dissolved in 2.72 mL of sulfuric acid and diluted to 10 mL with Milli-Q H2O to produce the titanium(IV) reagent with the final concentration of 100 mM Ti in 5 M H_2SO_4. Following DBD plasma treatment, 50 µL of the treated PBS sample was transferred into the cuvette and diluted with 150 µL of pristine PBS. 50 µL of an aqueous 80 mM solution of sodium azide (NaN_3) (S2002, Sigma-Aldrich) was added and mixed thoroughly, after which 50 µL of the titanium(IV) reagent were added. The solution was then placed in a sonicator (3200 ultrasonic bath, Branson) for 3-5 s to remove air bubbles. The cuvette was removed from the sonicator, wiped of water droplets, and read in the spectrophotometer at 400 nm. The quantitative analysis was performed using a calibration curve of H2O2 solutions with a range of defined concentrations as previously described.

4.1.2 NO_2^- and NO_3^-

A NO_2^-/NO_3^- colorimetric assay kit (780001, Cayman Chemical) was used for these experiments, following the developed protocols. NO_2^- was detected by adding 50 µL of Griess reagent 1 (sulphanilamide) to the DBD plasma-treated PBS in a 96-well plate, followed by immediately adding 50 µL of Griess reagent 2 (N-(1-naphthyl)ethylenediamine). In order to measure both NO_2^- and NO_3^-, a nitrate reductase mixture (780010, Cayman Chemical) and an enzyme cofactor mixture (780012, Cayman Chemical) were added to each sample and incubated

for 1 h before the Griess reagent steps, thus allowing for the conversion of NO_3^- into NO_2^-. Samples were prepared in triplicates, and the absorbance wavelength was measured in duplicates at 540 nm using a microplate reader (Infinite200 Pro, Tecan). Concentrations of NO_3^- and NO_2^- were calculated from a calibration curve, obtained using standard solutions provided in the assay kit.

4.1.3 $O/^1O_2/O_3$

The spin trap, 2,2,6,6-tetramethylpiperidine (TEMP) (115754, Sigma-Aldrich), was dissolved in PBS (50×10^{-3} M) and treated with DBD plasma. TEMP reacts with DBD plasma-generated $O/^1O_2/O_3$ to form the spin adduct 2,2,6,6-tetramethylpiperidine N-oxyl (TEMPO) [1, 2]. Immediately after DBD treatment, PBS was collected in 50 µL capillaries (Ringcaps) and TEMPO was analyzed with electron paramagnetic resonance spectroscopy analysis (MiniScope MS200 spectrometer, Magnettech). The EPR parameters were: 9.4 GHz frequency, 3.16 mW power, 100 kHz modulation frequency, 0.1 mT modulation amplitude, 30 s sweep time, 0.1 time constant, and 15 mT sweep width.

NaN_3 (S2002, Sigma-Aldrich) was added to the TEMP solution before DBD plasma treatment to quench $^1O_2$. In this case, the collected TEMPO spectrum would result from O/O_3. It must be acknowledged that in some cases, O_3 formed by plasma does not yield TEMPO due to its low amounts and its low diffusion into the liquid [3, 4]. However, at higher produced concentrations, O_3 was shown to react with TEMP to produce TEMPO [1]. The concentrations of the stable radical TEMPO reported here are a double integration of the simulated spectrum, as described elsewhere [5]. The simulations were performed using the hyperfine value (a_N=1.7 mT) from literature in the Spin Trap Database (National Institute of Environmental Health Sciences, 2018). The quantitative concentrations of TEMPO were obtained via a calibration of the EPR spectrometer with solutions of a stable radical 4-oxo-TEMPO (176141, Sigma-Aldrich) [6].

4.1.4 $ONOO^-$

A solution of 100 × 10^{-6} M L-tyrosine (T-3754, Sigma-Aldrich), 100 × 10^{-6} M diethylenetriaminepentaacetic acid (D1133, Sigma-Aldrich), and 2x PBS was made and treated with DBD plasma as described in previous reports. The solution was then immediately collected and flash frozen in liquid nitrogen. Plasma treatment of the solution would lead to the formation of the nitrated product, 3-nitrotyrosine, and liquid chromatography–mass spectrometry (LC–MS) was used to measure 3-nitrotyrosine as described elsewhere [7].

4.2 RONS Results

In the past, we have reported that the DBD plasma-generated species increased linearly with pulse frequency and treatment time [8]. This suggests that the number of pulses is directly responsible for the generation of RONS. To investigate this, four frequencies were tested (50, 100, 250, and 500 Hz) and the treatment time was adjusted to deliver the same number of pulses during DBD plasma treatment.

H_2O_2 was measured with UV–vis spectrophotometry (400 nm) from the reaction with potassium titanium(IV) oxalate solution and sodium azide (NaN_3). Treatment time ranged between 24─240 seconds in order to surpass the detection limit of the instrument; evaporation within this time frame was too low to be measured with our available analytical technique and thus considered negligible. It is clear that when pulses were standardized, the H_2O_2 concentration was equivalent (139.9 ± 26.6 µM), regardless of pulse frequency or treatment time (Figure 6a in the main paper).

All other species were measured with time frames between 10─100 seconds with a fixed number of 5000 pulses. NO_2^- and NO_3^- were measured with the Griess method and a nitrate reductase enzyme and cofactor. NO_3^- concentrations were calculated by subtracting the mean NO_2^- concentration of each treatment condition from the NO_2^- + NO_3^- concentrations. Here, the

concentrations of NO_2^- alone (35.5 ± 17.7 µM) and NO_3^- (128.9 ± 32.8 µM) were also equivalent when the number of pulses are standardized (Figure 6b in the main paper).

The TEMP spin trap was used to detect O, $^1O_2$, and O_3, which would interact and form stable nitroxide TEMPO. This product would be detected through EPR spectroscopy. The addition of NaN_3 was used as a selective scavenger of $^1O_2$ to estimate the relative amount of O and O_3 [9]. The addition of NaN_3 did not affect the measured amount of TEMPO (269.2 ± 64.2 µM) compared to that of TEMPO when NaN_3 was excluded (277.1 ± 46.2 µM). Therefore, this suggests that no considerable (i.e. detectable) amounts of $^1O_2$ were produced by plasma, and that the DBD plasma produced equivalent amounts of O/O_3 when the number of delivered pulses was fixed (Figure 6c in the main paper). We acknowledge that the absolute amounts of O/O_3 are likely dramatically higher than the respective amounts of the spin adduct TEMPO [2, 3, 9, 10]. However, the trends of the spin trapping results obtained under different conditions are expected to be similar to the trends of absolute concentrations of O/O_3 [2].

L-tyrosine in PBS was used to detect $ONOO^-$. DBD plasma treatment of the solution would form 3-nitrotyrosine, which was then measured with LC-MS with electrospray ionization. It is important to note that concentrations of $ONOO^-$ reported here may be an overestimation of the actual amount, as we have attributed the formation of 3-nitrotyrosine to $ONOO^-$ when in reality other species, such as $•NO_2$, could have also contributed. Equivalent amounts of 3-nitrotyrosine (3.52 ± 0.52 µM) were detected for all frequency treatments when the delivered DBD plasma pulses were fixed (Figure 6d in the main paper). Recent findings by Bruno et al. suggest that L-tyrosine tyrosine can also undergo multiple nitrations [11]. Because the employed method of nitrotyrosine detection did not include the products of such nitrations, it is also possible that we underestimate the amount of peroxynitrite. In any case, our results show that equivalent amounts

of 3-nitrotyrosine (3.52 ± 0.52 μM) were detected for all frequency treatments when the delivered DBD plasma pulses were fixed (Figure 6d in the main paper), regardless of the contribution of various RNS to the nitration of tyrosine.

It must be noted that with the exception of oxygen atoms, the RONS measured here are stable RONS, which persist in the plasma-treated PBS for a substantial amount of time after treatment (minutes to days). Some of these are formed in their molecular form in the gas phase plasma above the treated solution, while others are formed through the interaction of the short-lived radicals with the liquid H_2O [9, 12]. It is thus possible that $NO_2^-/NO_3^-/ONOO^-$ are formed in liquid from the $\bullet NO_x$ and •OH radicals which initially enter the solution from the gas phase. Although analysing the radical species could give additional information on their generation as a function of delivered energy, quantitative measurements of some radicals are not straightforward due to the limitations of the spin trapping techniques (e.g. •NO, •OH which we have only detected qualitatively [8]), such as the non-selectivity of spin traps and the decay of spin adducts [2, 13]. Therefore, in this work we focused on the long- and short-lived species for which detection methods enabled quantitative assessment.

Altogether, it is clear that for DBD plasma-generated species measured here, neither frequency nor application time alone was the major contributing parameter. Instead, the generation of RONS depended on the number of pulses delivered, which consequently is associated with the total delivered energy during plasma treatment.

REFERENCES

[1] N. Wardenier, Y. Gorbanev, I. Van Moer, A. Nikiforov, S.W. Van Hulle, P. Surmont, F. Lynen, C. Leys, A. Bogaerts, P. Vanraes, Removal of alachlor in water by non-thermal plasma: Reactive species and pathways in batch and continuous process, Water Res. 161 (2019) 549-559.
[2] Y. Gorbanev, A. Privat-Maldonado, A. Bogaerts, Analysis of short-lived reactive species in plasma–air–water systems: the dos and the do nots, ACS Publications, 2018.

[3] Y. Gorbanev, J. Van der Paal, W. Van Boxem, S. Dewilde, A. Bogaerts, Reaction of chloride anion with atomic oxygen in aqueous solutions: can cold plasma help in chemistry research?, PCCP 21 (2019) 4117-4121.
[4] D.T. Elg, I.-W. Yang, D.B. Graves, Production of TEMPO by O atoms in atmospheric pressure non-thermal plasma–liquid interactions, J. Phys. D: Appl. Phys. 50 (2017) 475201.
[5] A. Privat-Maldonado, Y. Gorbanev, S. Dewilde, E. Smits, A. Bogaerts, Reduction of human glioblastoma spheroids using cold atmospheric plasma: The combined effect of short-and long-lived reactive species, Cancers 10 (2018) 394.
[6] Y. Gorbanev, C. Verlackt, S. Tinck, E. Tuenter, K. Foubert, P. Cos, A. Bogaerts, Combining experimental and modelling approaches to study the sources of reactive species induced in water by the COST RF plasma jet, PCCP 20 (2018) 2797-2808.
[7] K. Wende, P. Williams, J. Dalluge, W. Van Gaens, H. Aboubakr, J. Bischof, T. Von Woedtke, S.M. Goyal, K.-D. Weltmann, A.J.B. Bogaerts, Identification of the biologically active liquid chemistry induced by a nonthermal atmospheric pressure plasma jet, 10 (2015) 029518.
[8] A. Lin, Y. Gorbanev, J. De Backer, J. Van Loenhout, W. Van Boxem, F. Lemière, P. Cos, S. Dewilde, E. Smits, A. Bogaerts, Non-Thermal plasma as a unique delivery system of short-lived reactive oxygen and nitrogen species for immunogenic cell death in melanoma cells, Advanced Science 6 (2019) 1802062.
[9] Y. Gorbanev, D. O'Connell, V. Chechik, Non-thermal plasma in contact with water: The origin of species, Chemistry–A European Journal 22 (2016) 3496-3505.
[10] B. Myers, P. Ranieri, T. Smirnova, P. Hewitt, D. Peterson, M.H. Quesada, E. Lenker, K.J.J.o.P.D.A.P. Stapelmann, Measuring plasma-generated· OH and O atoms in liquid using EPR spectroscopy and the non-selectivity of the HTA assay, 54 (2021) 145202.
[11] G. Bruno, S. Wenske, J.-W. Lackmann, M. Lalk, T.v. Woedtke, K.J.B. Wende, On the Liquid Chemistry of the Reactive Nitrogen Species Peroxynitrite and Nitrogen Dioxide Generated by Physical Plasmas, 10 (2020) 1687.
[12] Y. Gorbanev, R. Soriano, D. O'Connell, V. Chechik, An atmospheric pressure plasma setup to investigate the reactive species formation, JoVE (2016) e54765.
[13] Y. Gorbanev, N. Stehling, D. O'Connell, V. Chechik, Reactions of nitroxide radicals in aqueous solutions exposed to non-thermal plasma: limitations of spin trapping of the plasma induced species, Plasma Sources Science Technology 25 (2016) 055017.
[14] A. Lin, B. Truong, A. Pappas, L. Kirifides, A. Oubarri, S. Chen, S. Lin, D. Dobrynin, G. Fridman, A. Fridman, Uniform Nanosecond Pulsed Dielectric Barrier Discharge Plasma Enhances Anti-Tumor Effects by Induction of Immunogenic Cell Death in Tumors and Stimulation of Macrophages, Plasma Process Polym 12 (2015) 1392-1399.
[15] A. Lin, B. Truong, S. Patel, N. Kaushik, E.H. Choi, G. Fridman, A. Fridman, V. Miller, Nanosecond-Pulsed DBD Plasma-Generated Reactive Oxygen Species Trigger Immunogenic Cell Death in A549 Lung Carcinoma Cells through Intracellular Oxidative Stress, International Journal of Molecular Sciences 18 (2017) 966.
[16] A.G. Lin, B. Xiang, D.J. Merlino, T.R. Baybutt, J. Sahu, A. Fridman, A.E. Snook, V. Miller, Non-thermal plasma induces immunogenic cell death in vivo in murine CT26 colorectal tumors, Oncoimmunology 7 (2018) e1484978.
[17] O. Kepp, L. Senovilla, I. Vitale, E. Vacchelli, S. Adjemian, P. Agostinis, L. Apetoh, F. Aranda, V. Barnaba, N. Bloy, Consensus guidelines for the detection of immunogenic cell death, Oncoimmunology 3 (2014) e955691.

[18] L. Galluzzi, I. Vitale, S.A. Aaronson, J.M. Abrams, D. Adam, P. Agostinis, E.S. Alnemri, L. Altucci, I. Amelio, D.W. Andrews, Molecular mechanisms of cell death: Recommendations of the Nomenclature Committee on Cell Death 2018, Cell Death & Differentiation (2018) 1.